*Energy Science & Engineering*

WILEY

ORIGINAL ARTICLE OPEN ACCESS

# Synthesis of Carboxylic Cellulose Nanocrystals From Yellow Thatching Grass (*Hyparrhenia filipendula*) via Citric Acid Hydrolysis

Fildah Ayaa[1,2] | Michael Lubwama[1] | Samuel Ayodele Iwarere[2] | Michael Olawale Daramola[2] | John Baptist Kirabira[1]

[1]Department of Mechanical Engineering, School of Engineering, Makerere University, Kampala, Uganda | [2]Sustainable Energy and Environment Research Group, Department of Chemical Engineering, Faculty of Engineering, Built Environment and Information Technology, University of Pretoria, Hatfield campus, Pretoria, South Africa

**Correspondence:** Michael Olawale Daramola (Michael.Daramola@up.ac.za)

**Received:** 11 April 2025 | **Revised:** 3 November 2025 | **Accepted:** 11 December 2025

**Funding:** African center of excellence in Materials, product development and Nanotechnology; African Center of Excellence in Materials, Product Development and Nanotechnology (MAPRONANO ACE); World Bank and Government of Uganda, Grant/Award Number: P151847; IDA, Grant/Award Number: 5797-UG<!--Query ID="Q2" Text="AUTHOR: Please confirm or correct the Funding information as edited."-->; Prof. Daramola Development Fund

**Keywords:** biomass wastes | cellulose nanocrystals | citric acid | deep eutectic solvent | yellow thatching grass

## ABSTRACT

Grass is an abundant and renewable source of cellulose, which makes it a sustainable and cost-effective source for producing cellulose nanocrystals. Moreover, the extraction of cellulose nanocrystals from grass provides a value-added product from an otherwise low-value agricultural waste material, which can contribute to the development of a circular economy. In this study, cellulose nanocrystals (CNCs) were extracted from *Hyparrhenia filipendula* via citric acid hydrolysis. The *Hyparrhenia filipendula* stems were pre-processed through mechanical size reduction and Soxhlet extraction. The extractive-free stems were fractionated using two solvents: 10 wt% (w/v) sodium hydroxide (NaOH) and deep eutectic solvent of ethylene glycol:citric acid (1:2 molar ratio). The fractionated samples were bleached with acidified sodium chlorite and hydrolyzed with 80 wt% citric acid for 4 h at 120°C in a Parr reactor. The samples obtained at each treatment stage were characterized using standard scientific procedures for chemical composition, morphology, elemental composition, crystallinity, and thermal stability. The results show that CNCs were successfully extracted from *Hyparrhenia filipendula* via citric acid hydrolysis. The surface morphology of alkali fractionated CNCs was needle-like, whereas the surface morphology of DES fractionated CNCs was rod-like. The alkali fractionated and hydrolyzed sample, NaCNC, had the highest cellulose purity (91%), as well as the highest thermal stability. The FTIR analysis proved the removal of non-cellulosic components in the CNCs, except for the unbleached CNCs that had significant quantities of hemicellulose and lignin. The XRD analysis revealed the presence of characteristic cellulose Iβ in the CNCs, with the UNNaCNC sample (NaOH fractionated, unbleached, acid hydrolyzed sample) having the highest crystallinity index of 81% and the largest crystallite size of 4.20 nm. The properties of the CNCs obtained in this study are comparable to

**Abbreviations:** CNCs, cellulose nanocrystals; DES, deep eutectic solvent; DESCNC, CNC from DES pulping, acidified sodium chlorite bleaching, and citric acid hydrolysis; DES_B, pulped with des and bleached with acidified sodium chlorite; DES_P, pulped with deep eutectic solvent (DES); Dewaxed, extractive-free yellow thatching grass; NaCNC, CNC from NaOH pulping, acidified sodium chlorite bleaching, and citric acid hydrolysis; NaOH_B, pulped with sodium hydroxide and bleached with acidified sodium chlorite; NaOH_P, pulped with sodium hydroxide; Raw, dried and cleaned yellow thatching grass; UNDESCNC, CNC from DES pulping and citric acid hydrolysis (unbleached); UNNaCNC, CNC from NaOH pulping and citric acid hydrolysis (unbleached).

CNCs derived from previously reported lignocellulosic materials. The CNCs from *Hyparrhenia filipendula* therefore have a wide range of potential applications.

## 1 | Introduction

Cellulose is the most abundant polymer on earth [1–3]. Cellulose nanocrystals (CNCs) are highly crystalline renewable nanomaterials with at least one dimension equal to or less than 100 nm derived from lignocellulosic biomass [4–6]. CNCs are widely explored due to their unique properties, such as excellent mechanical properties, good biocompatibility, low density, biodegradability, non-toxicity, low cost, and colloidal stability [5, 6]. Additionally, CNCs also have various applications in Pharmaceuticals, biomedical devices, water purification technologies, packaging, food and cosmetics modifiers, and construction materials [7–10].

CNCs have been previously synthesized from several sources, such as wood, cotton, tunicates, and agricultural waste as documented elsewhere [11–14]. In this study, CNCs are extracted from yellow thatching grass (*Hyparrhenia filipendula*). Yellow thatching grass (*Hyparrhenia filipendula)* is a perennial grass widely distributed in East and Southern Africa [15]. Figure 1 depicts the geographical distribution of the grass in Africa. The grass is an invasive species and grows naturally in degraded soils. It is utilized for roofing houses and grazing cattle in its early stages of growth, but it is typically burned to control its growth and discarded [16]. This substrate is selected as a means of exploring cellulose-rich materials that do not interfere with food production, are readily available, and are easy to grow [17]. There are also no previous studies on the extraction, utilization, and commercial exploitation of *Hyparrhenia filipendula* for CNC production.

The main production method for CNCs is via acid hydrolysis, utilizing mineral acids like sulfuric acid, hydrochloric acid, and phosphoric acid. Organic acids such as maleic acid, formic acid, oxalic acid, and citric acid, however, have been increasingly used as part of efforts to minimize the impact of CNC production on the environment [18]. Previously, our research group synthesized cellulose nanofibers (CNFs) from yellow thatching grass via sulfuric acid hydrolysis [16]. In this work, CNCs are extracted from yellow thatching grass via citric acid hydrolysis. Citric acid is a tricarboxylic organic acid that is efficient in hydrolyzing lignocellulosic biomass with fewer degradation products and more oligomeric sugars, as reported by other authors [8, 19].

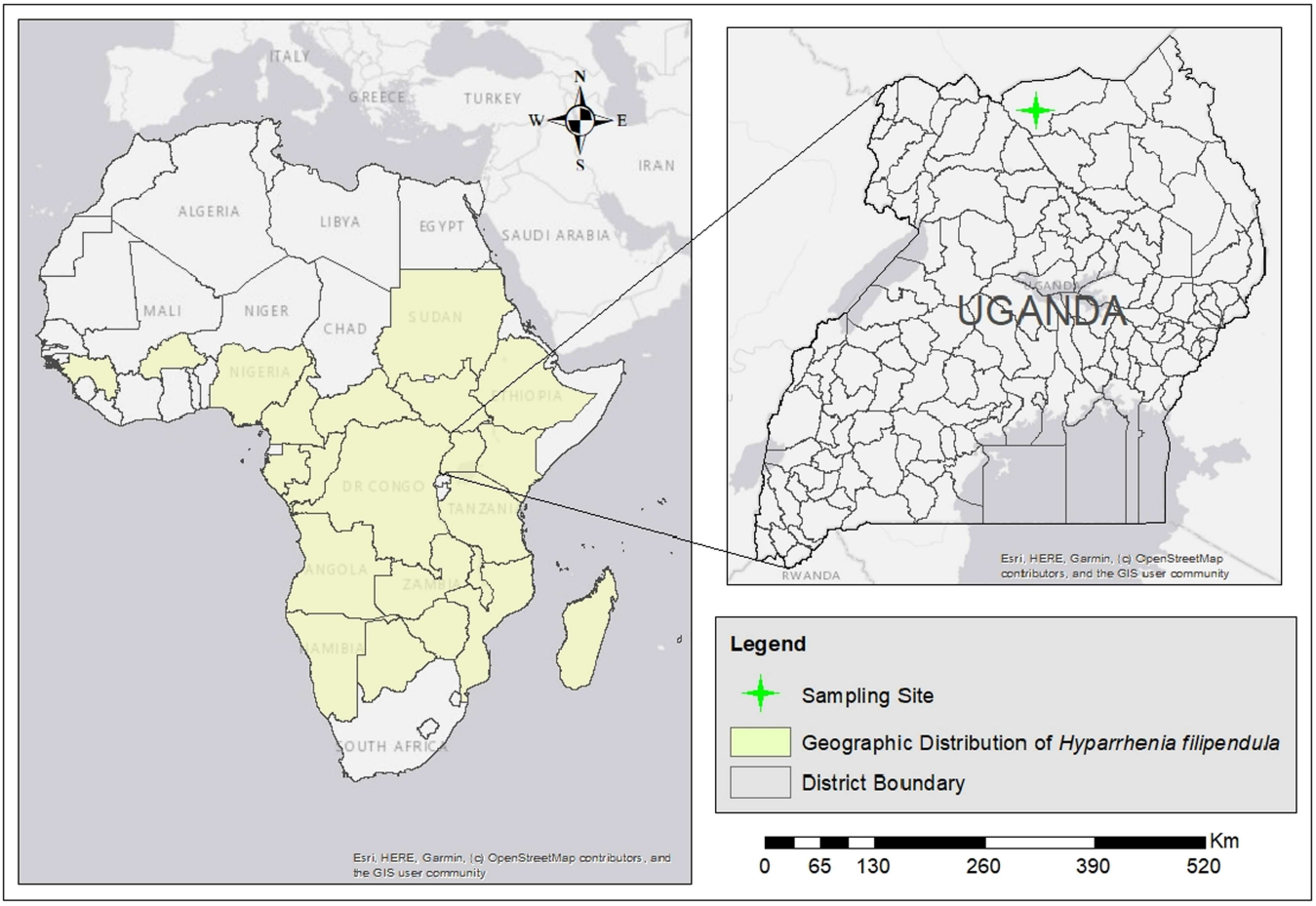


**FIGURE 1** | Geographical distribution of yellow thatching grass and sampling site for the study.

However, there are only a few limited studies reporting the use of Citric acid for CNC production [4, 20]. Bondancia et al prepared CNCs and CNFs from commercial eucalyptus cellulose pulp using 65 wt% citric acid at 120°C at different reaction times (1.5, 3, 4.5 and 6 h) in a homemade glass stirred reactor tank. The study concluded that it was possible to obtain CNCs and CNFs for all reaction times, but longer hydrolysis times resulted in more homogenous structures and higher yields of CNCs [21]. Similarly, Ji et al. synthesized CNCs and CNFs from bleached bagasse pulp using different concentrations of citric acid (60–80 wt%) at different reaction times (0.5–4 h) in a three-neck spherical flask. The yield of the CNCs obtained with a high concentration of citric acid (80%) and a longer hydrolysis time of 4 h was similar to the yields obtained using sulphuric acid [22]. Liu et al also confirmed that a citric acid concentration of 80 wt% and a temperature of 120°C or 140°C was needed to achieve sufficient hydrolysis for CNC production from commercial bleached softwood pulp in a Parr reactor [23]. Kassab et al. also synthesized CNCs from juncus plant stems using a 9:1 (v/v) citric acid (3 M)/hydrochloric acid (6 M) mixture for acid hydrolysis at 80°C for 4 h. The CNCs produced had a high thermal stability (>200°C) and high crystallinity of 83% with a cellulose I structure maintained [24]. Furthermore, Liu et al synthesized CNCs from bleached eucalyptus Kraft pulp using $FeCl_3$-catalyzed citric acid hydrolysis, at 100°C for 6 h in a flask [20]. The CNCs had a high crystallinity of 80% and high thermal stability [20]. However, our laboratory observations revealed that CNCs synthesized in a glass flask heated by an oil or water bath, or in an unlined stainless-steel autoclave, exhibited inferior quality compared to those produced in a Teflon-lined reactor or cup under identical experimental conditions. Additionally, the purity and quality of the acid used significantly influenced the physicochemical properties of the resulting CNCs.

The objective of this work, therefore, is to synthesize CNCs from *Hyparrhenia filipendula* via citric acid hydrolysis and to assess the influence of pretreatment, particularly during the pulping stage, on the resulting CNC properties. The biomass was pre-treated in two steps: fractionation and bleaching. The fractionation was carried out using alkali (NaOH) and deep eutectic solvent (DES) consisting of Ethylene glycol and citric acid. The DES system was previously reported to be efficient for delignification of paddy husks [7]. Also, DES solvents are classified as green solvents with selectivity for lignin, are inexpensive, easy to prepare, and non-flammable [25, 26]. Carboxylic acid-based DES systems have been reported to introduce carboxyl groups on the cellulose surface, improving the thermal stability and dispersibility of nanocellulose in aqueous solutions, which is conducive to its application in composite materials [27]. Moreover, sodium hydroxide is the most selective alkaline reagent for lignin and water-soluble hemicellulose removal in lignocellulosic biomass [28, 29]. The mechanism of sodium hydroxide treatment is reported by Modenbach & Nokes [30].

This work contributes to the development of pathways for the conversion of the *Hyparrhenia filipendula* stems into high-quality cellulose nanocrystals for different potential nanomaterial applications. To the best of our knowledge, the use of an acidic deep eutectic solvent (DES) composed of ethylene glycol and citric acid for pretreatment in nanocellulose extraction from this biomass has not been previously investigated, and unlike the commonly studied choline chloride-based DES systems, its impact on the resulting CNC properties remains unreported [31]. This work also presents a comparative analysis of fibers pretreated with sodium hydroxide (NaOH) versus those treated with the acidic DES. The morphology, size, physicochemical properties, crystallinity, and thermal stability of the resulting CNCs were analyzed.

## 2 | Materials and Methods

### 2.1 | Materials

The *Hyparrhenia filipendula* grass, locally known as "*Abili*" was harvested in the wild from Palabek Kal, Lamwo district, Uganda, in July 2022, as shown in Figure 1. The reagents; sodium hydroxide (Sigma-Aldrich, South Africa, 98%), toluene (Sigma-Aldrich, South Africa, 90%), acetic acid glacial (Sigma-Aldrich, South Africa, 99%), sodium chlorite (Sigma-Aldrich, South Africa, 80%), citric acid monohydrate (Glassworld, & Chemical Suppliers CC, Maraisburg, South Africa, 99.8%), ethylene glycol (Sigma-Aldrich, South Africa 99%), were used without further purification.

The Ethylene glycol/Citric acid (CA) DES was prepared using a molar concentration of 1:2 (EG:CA). This molar ratio was chosen in accordance with previous studies that reported the highest levels of delignification under similar conditions [7, 32]. The mixture was heated at 80°C, with constant magnetic stirring at 300 rpm, until a clear solution was formed. Once cooled to room temperature, the DES was stored in an airtight container for later use. The physicochemical properties of the DES are summarized in Table 1. The density was measured using an Attension Sigma force tensiometer (Sigma 700, Biolin Scientific USA). The conductivity was measured with a conductivity meter (Jenco Instruments 3020 M) and the dynamic viscosity with an RV-viscometer (NDJ-8S, W&J Instrument Co. Ltd, China).

### 2.2 | Synthesis of CNCS With NaOH

The *Hyparrhenia filipendula* grass was dried in the oven at 100°C for 2 h. The dried blades and sheaths were removed to expose the culm that was used in subsequent processes. The culm was cut into small pieces of lengths of about 1–2 cm, shredded in a blender, and milled using a PM 100 ball mill (Retsch, Germany) for 3 h, with 10 mm diameter stainless steel grinding balls at 300 rpm. The fibers were then passed through

**TABLE 1** | Physicochemical properties of deep eutectic solvent.

| Solvent | Density (g/mL) | Viscosity (mPa.s) | Conductivity (μS/cm) |
|---|---|---|---|
| Ethylene Glycol: Citric acid (1:2) | 1.50 ± 0.02 | 7532 ± 0.04 | 1334 ± 0.05 |

a 38 μm sieve and stored in an airtight container to prevent degradation of the sample. The extractives were removed using a Soxhlet extractor at 110°C for 4 h with toluene/ethanol (2:1 v/v). The extractive-free straws were then washed with de-ionized water and ethanol and dried at 45°C for 2 h.

The pulping of the extractive-free stems was carried out at 100°C for 4 h in a Parr reactor using 10 wt% NaOH and liquor- to -solid ratio of 15:1 (v/w). The pulp was extracted after the cooking time via vacuum filtration and washed several times with deionized water until a neutral pH was obtained. The pulp was then dried in the oven at 45°C for 2 h and stored for further analysis. 2 g of the pulp was then bleached using acidified sodium chlorite (1.2 g Sodium chlorite, 0.3 mL acetic acid, and 100 mL deionized water, pH 4.12) at 95°C for 4 h in a Parr reactor. The bleached pulp was washed with deionized water until a neutral pH was obtained. The filtrate was dried at 45°C for 1 h. The cellulose fibers were then hydrolyzed using 80 wt% citric acid (pH 1.06), with an acid-fiber ratio of 20:1 for 4 h in a Parr reactor at 120°C. The precipitate was dialyzed in deionized water for 3 days with up to four water changes per day, until a neutral pH was obtained. The sample was then sonicated in an ice bath for 2 h in a 480 W PS-80 Ultrasonic cleaner and homogenized using an HG-15D homogenizer at 10,000 rpm for 5 min. The sample was then frozen at −40°C for 12 h and freeze-dried for 72 h. The lyophilized CNCs were stored in an air-tight container for further analysis.

## 2.3 | Synthesis of CNCS With DES

DES was used to synthesize CNCs with minor changes to the process described in section 2.2. The sample is pulped with the DES using a liquor- to- solid ratio of 10:1 (v/w), and the pulp is washed with hot deionized water until a neutral pH is obtained. The bleaching and acid hydrolysis steps were not changed. The acidic DES is expected to facilitate the cleavage of β-O-4 ether and ester linkages in lignin and hemicellulose, resulting in lignin depolymerization and solubilization of hemicellulose [33–38].

## 2.4 | Synthesis of Unbleached CNCS

In contrast to the two previously described methods, the CNCs were synthesized without the bleaching step. The pulping and acid hydrolysis procedures remained unchanged. The mixture was then passed through a G1 sintered Buchner glass funnel to produce a concentrated suspension of unbleached CNCs. A summary of the synthesis routes for the CNCs is shown in Figure 2.

The nomenclature of the samples is as follows; Raw- dried and cleaned yellow thatching grass; Dewaxed- extractive-free yellow thatching grass; NaOH_P- pulped with sodium hydroxide; DES_P-pulped with DES solvent; NaOH_B- pulped with sodium hydroxide and bleached with acidified sodium chlorite; DES_P-pulped with DES and bleached with acidified sodium chlorite; NaCNC- CNC obtained from pulping with NaOH, bleaching

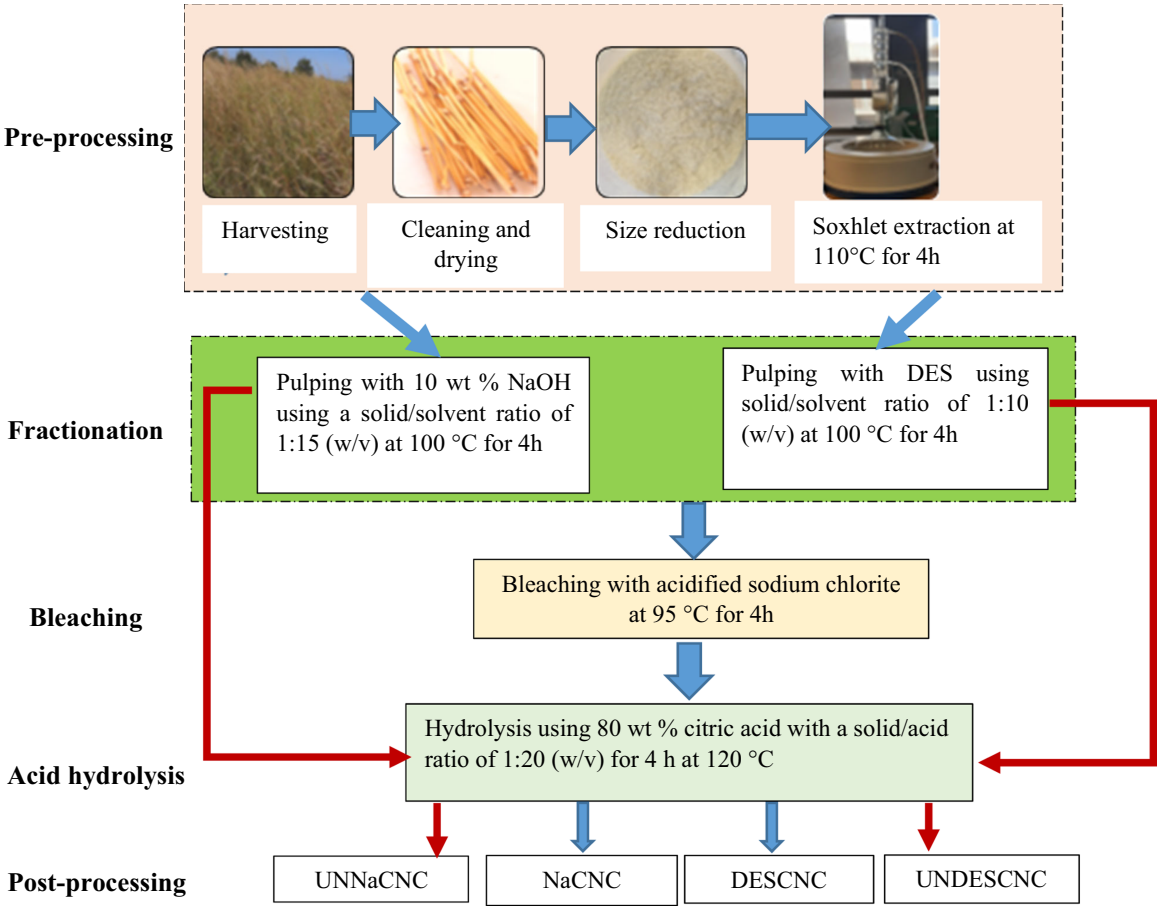


**FIGURE 2** | Synthesis routes for CNCs from yellow thatching grass.

with acidified sodium chlorite and hydrolysis with Citric acid; DESCNC- CNC obtained from pulping with DES, bleaching with acidified sodium chlorite and hydrolysis with Citric acid; UNNaCNC- CNC obtained from pulping with NaOH and hydrolysis with Citric acid; UNDESCNC- CNC obtained from pulping with DES and hydrolysis with Citric acid.

### 2.5 | Quantification of Carbohydrates and Lignin

A high-performance liquid chromatograph (Agilent 1260 Infinity, Germany) and a UV-visible Spectrophotometer (Hitachi U-3900 Spectrophotometer) were used to determine the carbohydrates and lignin in the sample using the procedure described by Sluiter et al. [39]. All measurements were done in triplicate, and the average is reported.

### 2.6 | Physicochemical Characterization of Samples

The morphology and elemental composition were examined using a transmission electron microscope (JEOL JEM 2100 F) and a Zeiss Ultra plus FEG Scanning electron microscope equipped with an energy dispersive X-ray spectroscope (EDS). A hypotonic suspension of the CNCs in ethanol was ultrasonicated for 12 h to avoid fiber aggregation during the TEM analysis. The samples for the SEM were coated with carbon using a Quorum Q150T ES sputter coater to enhance image resolution. Additionally, the samples were placed on a double-sided aluminum tape and coated with gold for the elemental analysis. The average elemental composition from ten sites on each sample is reported. The trace elements in the sample were analyzed with a Thermo Fisher ARL Perform'X sequential XRF spectrometer with Uniquant software. The thermal properties of the samples were determined by the ASTM E1131-08 standard procedure using a thermo gravimetric analyzer (HITACHI STA7300), with a flow of nitrogen of 10 mL/min, and a heating rate of 10°C/min. Functional groups in the samples were determined by Fourier Transform Infrared spectroscopy (FT-IR) in the medium infrared region of 4000–400 $cm^{-1}$ with a Bruker Alpha FTIR spectroscope. X-ray diffraction (XRD) analysis of the samples was conducted on a PANalytical X'Pert Pro powder diffractometer with Fe-filtered Co-Kα radiation ($\lambda = 1.789$ Å). The crystallinity index was obtained from Equation 1 [40]:

$$CI = 100 \times \frac{A_{crystalline}}{A_{crystalline} + A_{amophous}} \quad (1)$$

where $A_{amorphous}$ is the area under the amorphous curve, and $A_{crystalline}$ is the area under the sample curve.

The cellulose size was determined using Scherrer's equation as shown in Equation 2:

$$Crystalsize = \frac{k\lambda}{\beta \cos\theta} \quad (2)$$

Where $\lambda = 1.789$ nm, $k$ is the correction factor of 0.91, $\theta$ is the diffraction angle in radians, and $\beta$ is the full width at half maximum.

The d spacing of the cellulose nanocrystals was determined using Bragg's law, shown in Equation 3:

$$d = \frac{n\lambda}{2 \sin\theta} \quad (3)$$

where $d$ is the interplanar distance between lattice planes, $\theta$ is the scattering angle in degrees, $n$ is a positive integer, and λ is the wavelength of the X-ray.

## 3 | Results and Discussion

### 3.1 | Chemical Composition

The chemical composition of the samples at different treatment stages is shown in Table 2. The composition of the yellow thatching grass is comparable to other grass species previously reported in literature [41, 42]. The extractives in the yellow thatching grass are approximately 16%, comparable to other previously reported grass species such as *Agropyron repens L.*(16%), *Arrhenatherum elatius* (15%), and *paspalum* (15%) [43, 44]. Approximately 1% of extractives were not removed from the yellow thatching grass after Soxhlet extraction.

**TABLE 2** | Chemical composition of *Hyparrhenia filipendula* and derived CNCs.

| Sample | Composition % | | | Acid insoluble Ash | Others[a] |
|---|---|---|---|---|---|
| | Cellulose | Hemicellulose | Lignin | | |
| Raw | 34.14 ± 0.68 | 26.36 ± 3.11 | 22.35 ± 0.29 | 1.44 ± 0.00 | 15.71 ± 0.00 |
| Dewaxed | 39.87 ± 0.28 | 31.49 ± 0.32 | 25.89 ± 1.34 | 1.72 ± 0.00 | 1.03 ± 0.00 |
| NaOH_ P | 83.58 ± 1.12 | 6.58 ± 1.61 | 9.84 ± 0.02 | — | — |
| DES_ P | 59.10 ± 0.28 | 11.10 ± 0.92 | 25.24 ± 0.17 | 4.56 ± 0.00 | — |
| NaOH_ B | 93.25 ± 0.93 | 3.93 ± 0.90 | 2.82 ± 1.90 | — | — |
| DES_ B | 65.02 ± 0.39 | 28.03 ± 0.45 | 5.79 ± 0.64 | 1.16 ± 0.00 | — |
| NaCNC | 91.39 ± 1.25 | 5.21 ± 0.75 | 3.40 ± 0.89 | — | — |
| DESCNC | 83.19 ± 0.12 | 13.27 ± 0.28 | 3.54 ± 1.18 | — | — |
| UNNaCNC | 79.04 ± 0.98 | 9.94 ± 1.49 | 10.81 ± 0.17 | 0.21 ± 0.00 | — |
| UNDESCNC | 68.32 ± 0.45 | 15.63 ± 0.91 | 12.67 ± 0.22 | 3.38 ± 0.00 | — |

[a]Others may contain organic compounds (proteins, resins, and gums), waxes, and fats

Consequently, the dewaxed sample has a higher lignin value than the raw sample because unhydrolyzed carbohydrates condense with acid-insoluble lignin if extractable material is not fully removed [39]. A significant delignification of 62% was achieved after pulping with sodium hydroxide, while only 3% delignification was achieved with the DES. Alkaline delignification has been previously reported to be effective because the ester bond between the ferulic acid and carbohydrates is highly susceptible to alkali degradation, as the hydroxide ion increases the rate at which the irreversible hydrolysis reaction occurs [30, 45]. According to Okur and Koyuncu [7], the hydrogen bond interactions in the DES decrease at high temperatures, decreasing its viscosity, allowing the DES to penetrate in the biomass more easily and break the bonds between lignin, hemicellulose, and cellulose. Therefore, to achieve a higher delignification with the DES, a higher temperature is recommended for the fractionation process. However, a comprehensive understanding of how DES composition and physicochemical properties influence the selective fractionation of biopolymers remains lacking, despite a predicted reaction mechanism indicating that lignin exhibits significant recalcitrance in the presence of the DES [46]. This DES appears to be most effective for hemicellulose solubilization, as illustrated by the compositional analysis of the DES-pulped sample presented in Table 2. A comprehensive comparison of the chemical composition of biomass pretreated with similar DES systems is also available in the literature [47–49].

Additionally, the lignin content of the raw yellow thatching grass was 22%, and it decreased to approximately 3% and 6% after bleaching for NaOH_B and DES_B samples, respectively. The bleached pulps also showed a high cellulose purity (93% and 65% for NaOH_ B and DES_B, respectively) compared to the raw sample (34%). The cellulose purity attained for NaOH_B is comparable to commercial grade cellulose, which has cellulose content of 85%, hemicellulose content of 12%, and lignin content of 3%, as previously reported in literature [50].

The cellulose content also increased with chemical treatment, as expected. Notably, the cellulose content of NaCNC is 2% lower than that of NaOH_B due to possible cellulose degradation caused by hydrolytic cleavage of polymer glycosidic linkages occurring within accessible regions of the molecules [51]. The cellulose purity of the unbleached CNCs was also lower than that of their corresponding bleached counterparts, as expected due to persistence of non-cellulosic components, in agreement with other studies [52].

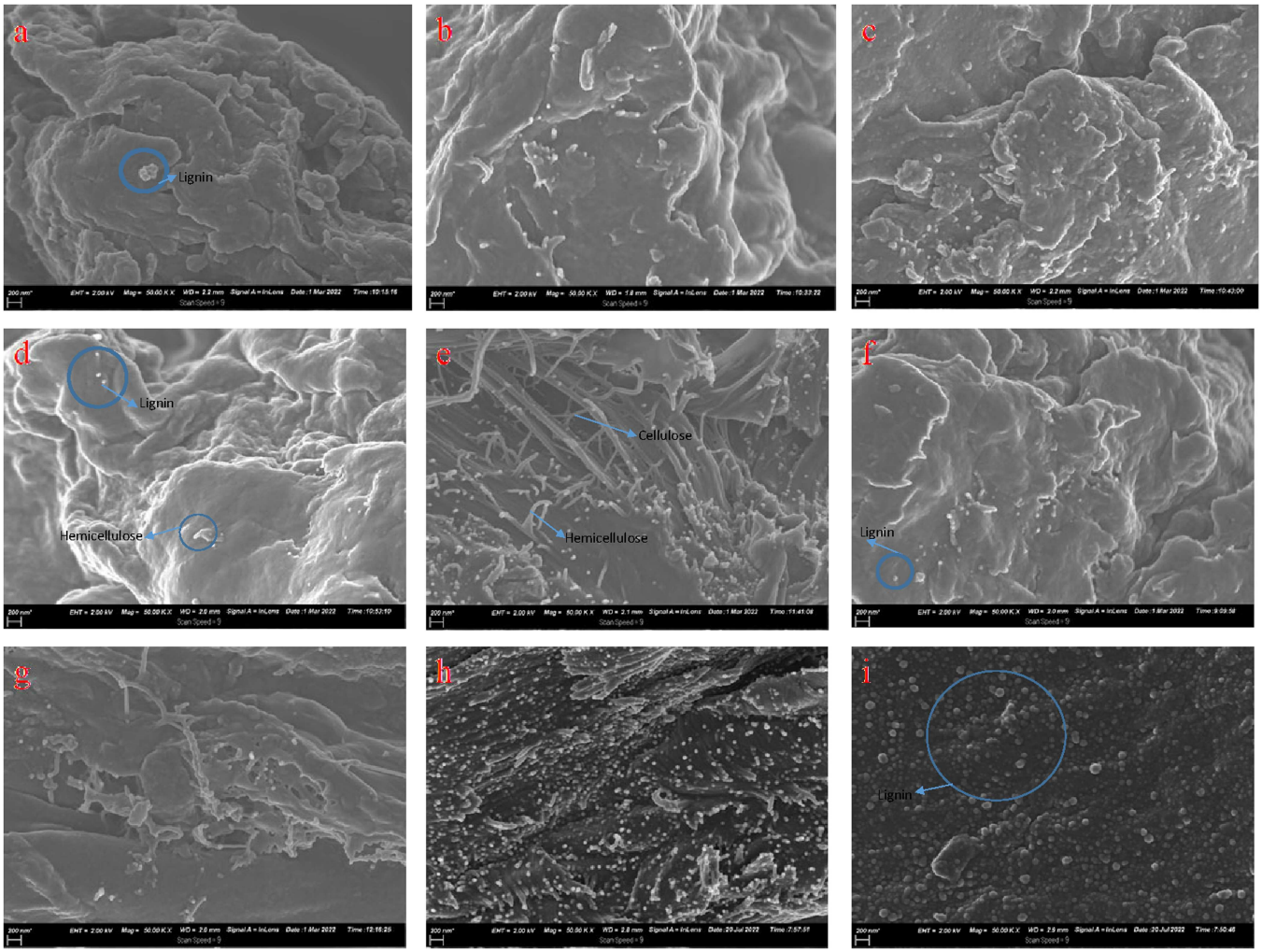


**FIGURE 3** | Morphology of (a) raw thatching grass; (b) NaOH_P (c) DES_P (d) NaOH_B (e) DES_B (f) NaCNC (g) DESCNC (h) UNNaCNC (i) UNDESCNC. Morphology of yellow thatching grass, intermediate products, and CNCs.

### 3.2 | Morphology

The morphology of the yellow thatching grass before and after processing is shown in Figure 3. The micrograph of the raw sample surface reveals an intact fiber with clusters of lignin on it. Compared to the DES_P sample, the NaOH_P sample had less lignin on its surface, supporting the findings of the chemical analysis in Table 1. When the melting temperature of lignin is exceeded during the pulping process, it is redeposited as droplets on the surface walls of the pulped samples. Additionally, the hemicellulose short chains in the DES_P sample were less exposed, indicating that lignin and hemicellulose were likely still more interconnected.

The surface of the NaOH_B sample is corrugated and sheet-like, indicating exposed cellulose bundles associated with the self-assembly behavior of cellulose. This is caused by the strong hydrogen bonding between cellulose sub-units that likely occurs during freeze-drying of the samples [53]. In contrast, the DES_B sample has multiple exposed short chains of hemicellulose, interwoven cellulose fibrils, and lignin deposits. The fact that the DES_B fiber is still largely intact suggests that the bleaching process did not effectively depolymerize hemicellulose and lignin in the sample.

Further still, the surface structure of NaCNC is similar to NaOH_B, exhibiting more pronouncedly swollen crystalline cellulose regions [54]. Relative to DES_B, DESCNC features more serrated exposed cellulose bundles, and fewer lignin deposits and hemicellulose chains, in agreement with the chemical composition in Table 1. Although UNNaCNC has more exposed bundles of cellulose than UNDESCNC, both of the unbleached CNCs' surfaces exhibit substantial lignin deposits.

The TEM images in Figure 4 confirm the extraction of CNCs from yellow thatching grass. NaCNC and UNNaCNC have a needle-like structure typical of cellulose nanocrystals [55–57]. On the other hand, DESCNC and UNDESCNC feature a rod-like morphology with an internal hollow bamboo architecture. The needle-shaped CNCs tend to form web-like structures that enhance the physical properties of the composites, while the rod-like structures confirm the efficiency of mild extraction with DES fractionation that result in highly crystalline entities [58]. The average diameters of the CNCs is summarized in Table 3. The acid hydrolysis treatment is expected to cleave the amorphous region of the CNCs transversely while leaving the crystalline domains intact. This in turn reduces the size of the CNCs to the nanometer scale [59].

**TABLE 3** | Average diameter of extracted CNCs.

| Sample | Average diameter, nm |
|---|---|
| NaCNC | $18 \pm 4.44$ |
| DESCNC | $22 \pm 6.81$ |
| UNNaCNC | $12.35 \pm 3.86$ |
| UNDESCNC | $40 \pm 6.46$ |

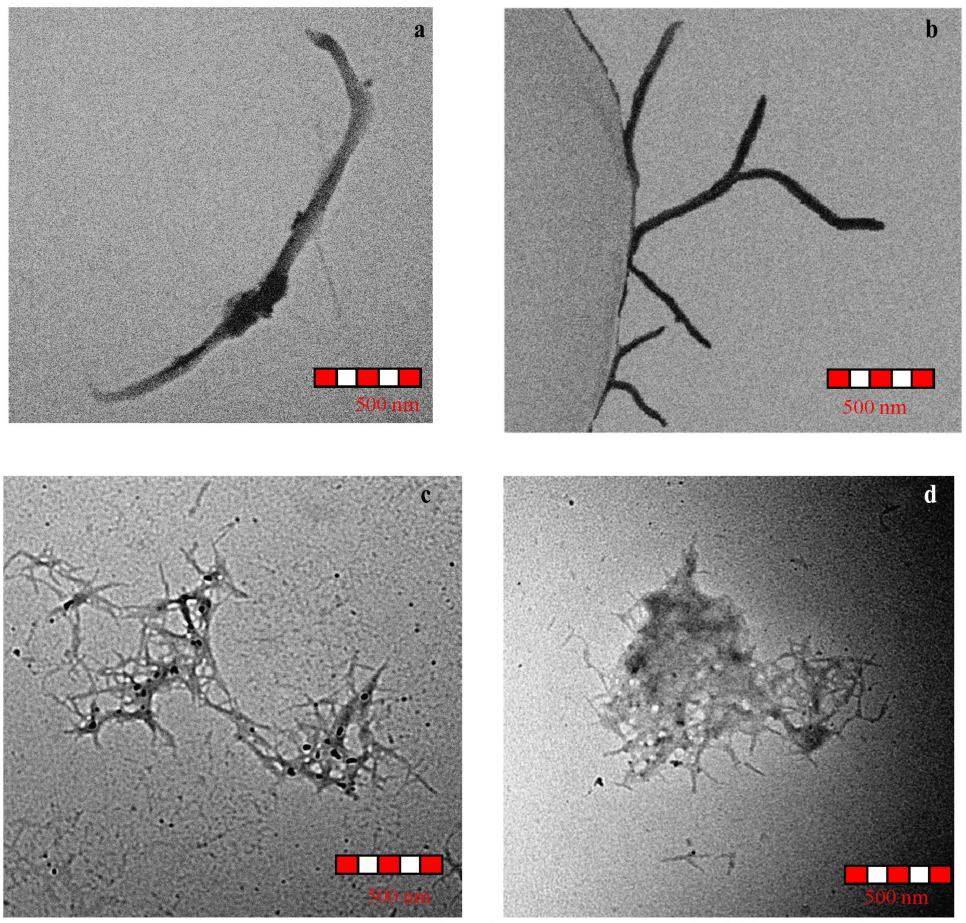


**FIGURE 4** | TEM images for (a) DESCNC; (b) UNDESCNC (c) NaCNC (d) UNNaCNC.

The diameters of the CNCs are comparable to those previously reported for CNFs/CNCs from grasses: Napier fiber (16.10–167.6 nm); Jute (15–25 nm); marram grass (4–5 nm); and Australian desert grass (16–32.2 nm) [55, 60, 61]. However, CNCs that appear as distinct particles may really consist of two lateral main crystallites that cannot be distinguished by either TEM or atomic force microscopy, according to Chen et al. [62]. The crystallites may be linked by amorphous cellulose that is not removed during the acid hydrolysis or may be initially separated particles that are strongly hydrogen bonded [62].

### 3.3 | Elemental Composition

The elemental analysis of the samples is shown in Table 4. The carbon content of the samples is in the range between 66% and 80%. Also, the oxygen content of the samples is in the range between 16% and 33%. The increased oxygen content observed in the treated samples most likely indicates the presence of C-O, C-C, O-C- O, C=O, O-C=O, and C-OH groups on the surface of the samples [45]. The alkali pulped sample, NaOH_P, has the lowest Silicon content, confirming the results from the morphology, where the sample had a completely fragmented

**TABLE 4** | Elemental analysis of samples.

| | Element, wt% | | | | | |
|---|---|---|---|---|---|---|
| **Sample** | **C** | **O** | **Si** | **Ca** | **Na** | **Mg** |
| Raw | 74.86 ± 3.25 | 21.64 ± 0.94 | 3.29 ± 3.01 | 0.22 ± 0.25 | — | — |
| NaOH_ P | 65.71 ± 3.26 | 32.90 ± 3.28 | 0.42 ± 0.10 | 0.19 ± 0.13 | 0.49 ± 0.16 | 0.29 ± 0.08 |
| DES_P | 76.80 ± 6.16 | 20.26 ± 3.22 | 2.93 ± 3.03 | — | — | — |
| NaOH_B | 68.65 ± 2.01 | 31.31 ± 2.06 | — | 0.05 ± 0.08 | — | — |
| DES_B | 76.35 ± 1.89 | 23.65 ± 1.89 | — | — | — | — |
| NaCNC | 76.22 ± 2.38 | 23.78 ± 2.38 | — | — | — | — |
| DESCNC | 72.63 ± 1.81 | 23.57 ± 1.74 | 3.80 ± 1.96 | — | — | — |
| UNNaCNC | 79.78 ± 1.41 | 19.07 ± 1.38 | — | 0.43 ± 0.12 | 0.73 ± 0.12 | — |
| UNDESCNC | 80.04 ± 1.53 | 16.60 ± 1.07 | 3.19 ± 0.95 | 0.17 ± 0.02 | — | — |

**TABLE 5** | Trace elements in selected samples.

| | **RAW** | **UNDESCNC** | **DESCNC** | **UNNaCNC** | **NaCNC** |
|---|---|---|---|---|---|
| **Si** | 4.26 | 2.44 | 2.83 | 0.04 | 0.04 |
| **Al** | < 0.01 | < 0.01 | < 0.01 | < 0.01 | < 0.01 |
| **Mg** | 0.12 | 0.10 | 0.01 | 0.08 | 0.04 |
| **Na** | < 0.01 | 0.03 | < 0.01 | 0.24 | 0.03 |
| **P** | 0.20 | < 0.01 | < 0.01 | < 0.01 | < 0.01 |
| **Fe** | 0.01 | 0.01 | 0.01 | 0.21 | 0.02 |
| **K** | 0.64 | 0.01 | < 0.01 | 0.01 | 0.01 |
| **Ca** | 0.10 | 0.11 | < 0.01 | 0.18 | 0.04 |
| **Zr** | < 0.01 | < 0.01 | < 0.01 | < 0.01 | < 0.01 |
| **Cr** | < 0.01 | < 0.01 | < 0.01 | 0.06 | < 0.01 |
| **S** | 0.01 | 0.01 | < 0.01 | < 0.01 | < 0.01 |
| **Cl** | 0.06 | 0.01 | 0.05 | < 0.01 | 0.02 |
| **Ni** | — | < 0.01 | < 0.01 | 0.02 | < 0.01 |
| **Zn** | — | < 0.01 | < 0.01 | 0.01 | < 0.01 |
| **Cu** | — | < 0.01 | < 0.01 | 0.01 | < 0.01 |
| **Mn** | — | < 0.01 | < 0.01 | 0.01 | < 0.01 |
| **Ba** | 0.10 | — | — | — | — |
| **I** | 0.04 | — | — | — | — |
| **Cs** | < 0.01 | — | — | — | — |
| **W** | < 0.01 | — | — | — | — |
| **Cellulose rest%** | 94.38 | 97.13 | 96.95 | 99.01 | 99.61 |
| **TOTAL** | **99.91** | **99.84** | **99.84** | **99.89** | **99.82** |

*Note:* Bold values is for emphasis of the total elements and cellulose detected with the XRF.

surface. The Silicon content of the DES_P sample is comparable to the raw sample, indicating that the structure was mostly unaltered during treatment. The presence of Silicon in plant material is problematic in industrial utilization of biomass as it forms insoluble precipitates and causes wear of equipment. Cell-wall-bound Silicon also affects the composition of plant cell walls by altering the linkages of non-cellulosic polymers and lignin [63].

The increase in the concentration of trace elements such as Na in processed samples, on the other hand, is due to the introduction of these elements from the reagents employed to process the sample [64].

### 3.4 | Trace Elements in CNCS

The trace elements in the CNCs were further examined by X-ray fluorescence (XRF) because the detection limit of XRF is better than that of EDS [65]. The results in Table 5, for example, show a small amount of Si, Cl, Mg, Ca in NaCNC and UNNaCNC that were not originally detected in the EDX test. In comparison to the raw sample, the CNC samples have a much lower concentration of the majority of trace elements due to the thermochemical processing. The trace elements present in yellow thatching grass are also comparable to other grass species like Eri and Loudetia grass, although the compositions vary due to differences in the grass species, phonological stage and environmental conditions in the eco-system [66–69].

### 3.5 | Surface Chemistry of the CNCS

The changes in the surface chemistry of the samples is illustrated by the FTIR spectra in Figure 5 and the main peaks summarized in Table 6. All the spectra display the typical peaks for lignocellulosic biomass along with variations in wavenumber and absorption intensity in the fingerprint and functional group regions for the samples. The fingerprint region in particular is characterized by the appearance and disappearance of some peaks as shown in Table 6 in line with observations from other authors [10, 70–77]. The peak at 1735 $cm^{-1}$ is assigned to the radical of C=O, that is either for the ester carbonyl group or carboxylic group from cellulose esterification by citric acid [22, 78]. This peak was only dominant in the UNNaCNC sample, although it was expected to appear in all the CNC samples. This is probably because UNNaCNC has the smallest particle size, as shown in Table 3, thus having a larger contact surface area to undergo the esterification reaction with citric acid [22, 79]. Furthermore, absorption between 1750 and 1700 $cm^{-1}$ also indicates the presence of a carbonyl compound such as a ketone, aldehyde, ester, or carboxylic acid [80, 81]. Absorption between 1650 and 1600 $cm^{-1}$ further confirms the presence of these groups due to a conjugated double bond [57, 80]. These absorptions were observed for all the CNCs, as shown in Table 6, which would indicate successful carboxylation of the CNCs. A conductometric titration test is however required to further investigate the extent of carboxylation of the CNCs.

### 3.6 | Crystallinity of CNCS

The X-ray diffraction (XRD) pattern of the raw and extracted CNCs is shown in Figure 6, and the crystallinity index is in Table 7. The XRD pattern for all samples is typical of the cellulose I polymorph as observed by other authors [82]. The major crystalline peak was observed at approximately $2\theta = 26$ ° for all the samples, showing that the native cellulose crystal $I_\beta$ structure was preserved [23]. The presence of a peak at $2\theta = 14°$ and a shoulder peak at $2\theta = 24°$ in NaCNC and UNNaCNC samples shows the presence of cellulose II polymorph. The existence of the cellulose II structure indicates that cellulose is dissolved and regenerated by the citric acid [70]. The peaks are also observed at higher angles due to the nature of the cellulose (some persistent lignin and trace elements, as shown in Tables 2 and 5). Also, the removal of lignin and hemicellulose in the sample changes the hydrogen bond between the cellulose chains, causing a slight change in the position of the peaks [77]. Furthermore, these peaks are speculated to be the result of graphitic structures forming from prolonged exposure to high

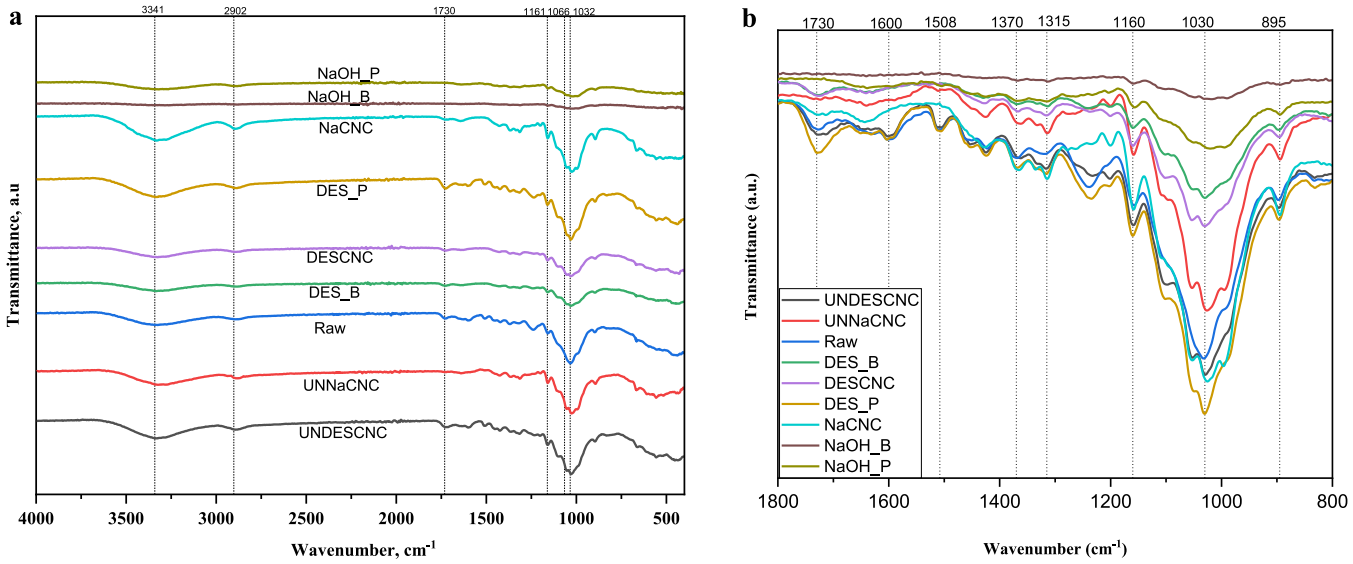


**FIGURE 5** | FTIR Spectra (a) entire spectra and (b) fingerprint region recorded for selected samples.

**TABLE 6** | Selected major peak transmittance positions for samples.

| Peak positions, $cm^{-1}$ | | | | | | | | | |
|---|---|---|---|---|---|---|---|---|---|
| **Raw** | **NaOH_ P** | **DES_ P** | **NaOH_ B** | **DES_B** | **NaCNC** | **DESCNC** | **UNNaCNC** | **UNDESCNC** | **Functional group** |
| 3325 | 3390-3186 (broad peak) | 3332 | 3400-3184 (broad peak) | 3333 | 3331 | 3325 | 3333-3266 (broad peak) | 3333 | Hydroxyl groups (O-H stretching vibration) related to cellulose |
| 2888 | 2889 | 2885 | 2874 | 2887 | 2896 | 2890 | 2887 | 2896 | C–H symmetrical stretching of cellulose and hemicellulose |
| 1727 | — | 1729 | — | 1727 | — | 1727 | 1722 | 1716 | Acetyl or uronic ester groups of hemicelluloses in the region 1700–1740 $cm^{-1}$, and the absence of this band indicates the removal of hemicelluloses |
| — | — | — | — | — | — | — | 1735 | — | Presence of carboxylic acid groups |
| — | — | — | — | — | — | — | — | 1730 | C = O stretching of the acetyl and urate groups of hemicellulose, or the ester bond of carboxyl groups in lignin to fragrant acid and ferulic acid |
| 1629 | 1639 | — | 1641 | — | 1644 | 1641 | 1642 | 1644 | Conversion from cellulose I to cellulose II |
| 1602 | — | 1603 | 1608 | — | — | — | — | 1602 | Aromatic skeletal vibration due to the presence of lignin and $COO^{-}$ stretching due to the presence of hemicellulose in the region 1600 $cm^{-1}$ |
| 1510 | 1505 | 1506 | — | — | — | — | 1513 | 1510 | C=C symmetrical stretching of aromatic rings that are typical of lignin |
| 1032 | — | 1031 | — | 1030 | 1026 | 1030 | 1027 | 1028 | C–C, C–OH, and C–H ring and side group stretching vibrations attributed to cellulose (dominant) and lignin. The highest intensity observed for NaOH_B, which had the highest amount of cellulose |
| 898 | 894 | 897 | 894 | 897 | 895 | 896 | 891 | 894 | C—H rock vibration of cellulose (anomeric vibration, specific for β-glucosides) |

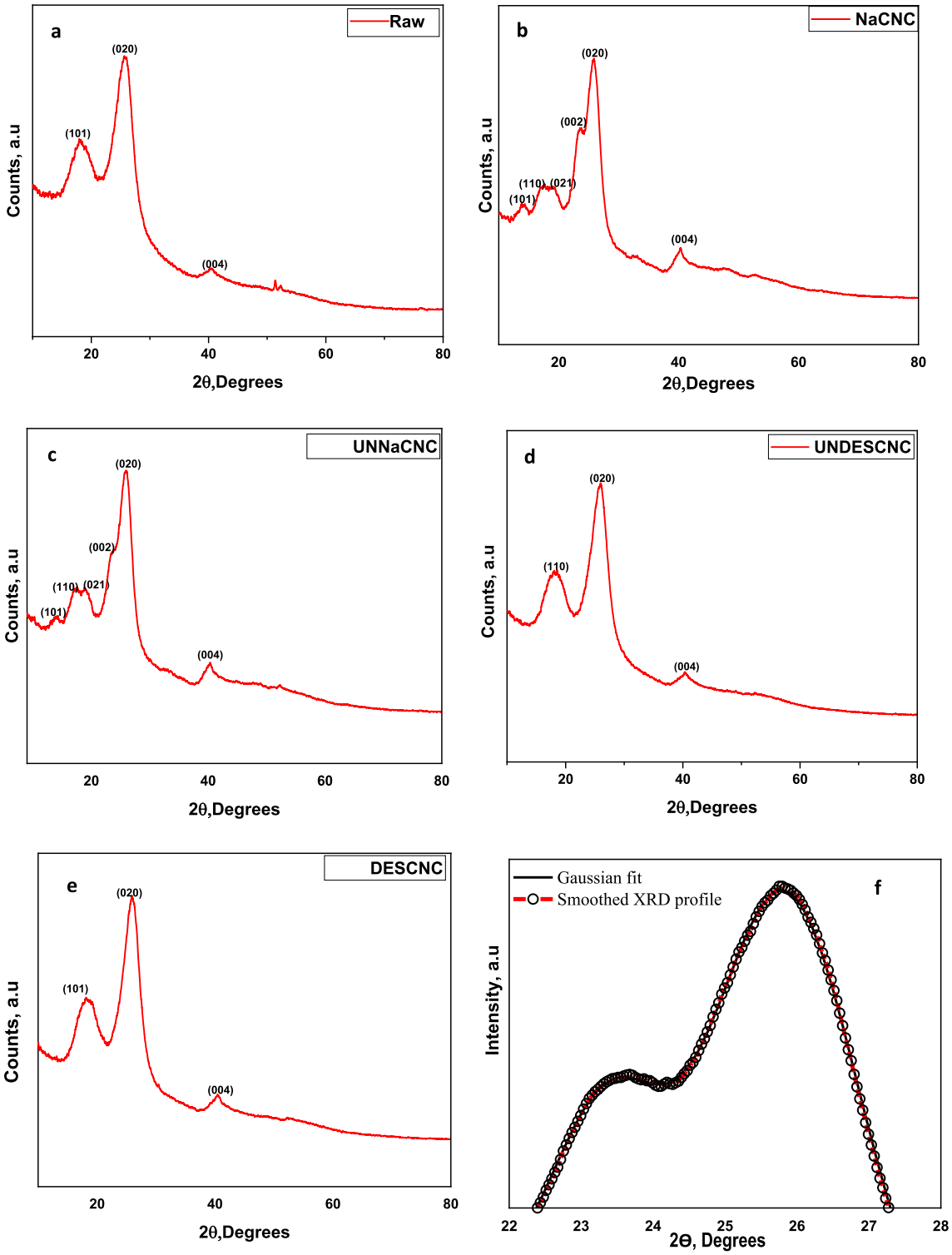


**FIGURE 6** | X-ray diffraction patterns of (a) Untreated sample; (b) NaCNC; (c) UNNaCNC; (d) UNDESCNC; (e) DESCNC; (f) Example of Gaussian fit for XRD profiles used in this study.

acidity or pseudolignin deposition as seen in the SEM images [83].

Additionally, the intensity of the crystallinity peaks decreased in the following order: NaCNC, UNNaCNC, DESCNC, UN-DESCNC, and raw sample. The bleached CNCs had higher intensity peaks and crystallite size than their unbleached counterparts due to chemical purification as noted by other authors [77, 84]. However, the crystallite size is 3-10 times smaller than the diameter measured from the TEM analysis in Table 3, due to the presence of aggregated and individual CNCs after freeze-drying as noted by other authors [40, 62]. The crystallite size and crystallinity index are also compared to previously derived CNCs from other sources, as shown in Table 7. However, the degree of crystallinity of nanocellulose

**TABLE 7** | Crystallinity index and size of cellulose nanocrystals from yellow thatching grass.

| Sample | Crystallite size, nm | *d* spacing, nm | Crystallinity index, % | Reference |
|---|---|---|---|---|
| **Raw** | 3.88 | 0.351 | 79 | This study |
| NaCNC | 4.14 | 0.356 | 80 | This study |
| DESCNC | 4.06 | 0.354 | 76 | This study |
| UNNaCNC | 4.20 | 0.355 | 81 | This study |
| UNDESCNC | 4.01 | 0.353 | 77 | This study |
| CNC from jackfruit peels | 2.80 | 0.21 | 83 | [40] |
| Commercial CNC | 4.4 | — | 85 | [82] |
| Bacterial cellulose | 6.5 | — | 70 | [72] |

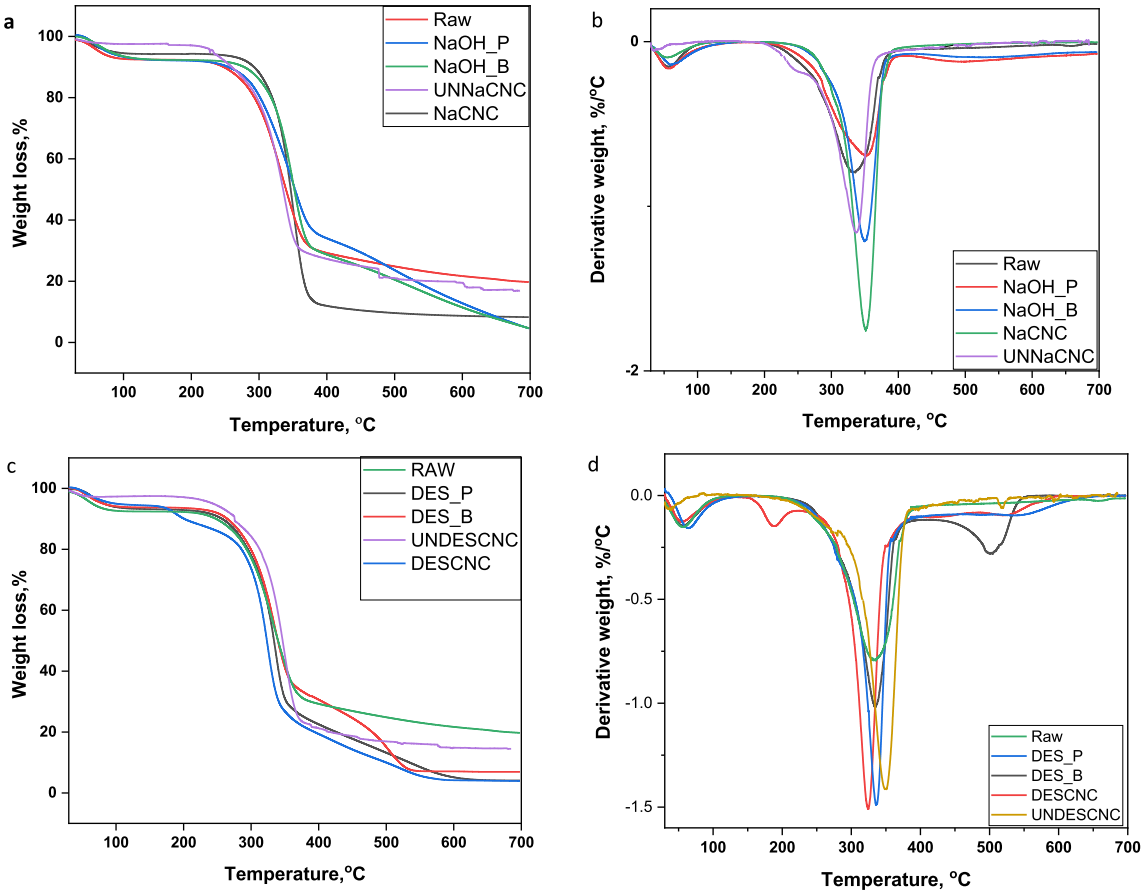


**FIGURE 7** | TGA and DTG curves for all samples; (a) TGA profile for samples and CNCs pulped with NaOH. (b) DTG profile for samples and CNCs pulped with NaOH. (c) TGA profile for samples and CNCs pulped with DES. (d) DTG profile for samples and CNCs pulped with DES.

also depends on the cellulosic raw material, as noted by other authors [85]. The decrease in the crystallite size of the bleached CNCs in comparison to the unbleached CNCs is associated with the strong hydrolysis at both a high temperature and reaction time that eliminated the amorphous components and even portions of the crystalline component, producing the reduced crystallite sizes and crystallinity [84]. To increase the crystallinity of the CNCs, the acid hydrolysis conditions must consequently be optimized. The crystallinity of the CNCs obtained from the sodium hydroxide and deep eutectic solvent pretreatments is comparable to values reported in literature [78, 86–88].

## 3.7 | Thermal Stability

The thermogravimetry (TG) curves and derivative thermogravimetry (DTG) curves for all the samples are depicted in Figure 7, and a summary of the weight loss, onset temperature ($T_i$), final temperature ($T_f$), and peak temperature ($T_p$) of the two stages of thermal decomposition is in Table 8. The weight loss within the temperature range of 29°C–101°C is associated with evaporation of intermolecular hydrogen-bonded water, free moisture, or degradation of low molecular weight compounds in the sample [77, 90]. The UNNaCNC sample exhibited the least weight loss in this temperature range due to its high crystallinity, as shown in Table 7 [84].

**TABLE 8** | Summary of TGA data.

| Samples | Moisture loss | | | Thermal decomposition | | | | Residual char, % | Reference |
|---|---|---|---|---|---|---|---|---|---|
| | $\Delta m$, % | $T_i$,°C | $T_f$,°C | $\Delta m$, % | $T_i$,°C | $T_f$,°C | $T_p$,°C | | |
| **Raw** | 6.46 | 38.43 | 86.81 | 72.98 | 314.49 | 369.78 | 331.23 | 19.71 | This study |
| NaOH_P | 8.36 | 37.99 | 101.82 | 87.39 | 275.19 | 449.35 | 348.94 | 4.58 | |
| NaOH_B | 7.88 | 40.96 | 101.22 | 87.97 | 304.10 | 421.71 | 348.75 | 4.50 | |
| NaCNC | 4.65 | 37.99 | 81.74 | 85.47 | 304.02 | 404.16 | 350.64 | 8.26 | |
| UNNaCNC | 1.49 | 28.71 | 81.17 | 79.65 | 221.59 | 381.12 | 338.89 | 16.91 | |
| DES_P | 6.40 | 46.17 | 92.20 | 89.08 | 292.45 | 383.67 | 336.91 | 4.09 | |
| DES_B | 6.47 | 40.27 | 87.15 | 87.39 | 290.21 | 389.43 | 336.82 | 6.912 | |
| DESCNC | 5.62 | 42.88 | 85.33 | 89.92 | 280.95 | 366.27 | 325.17 | 3.98 | |
| UNDESCNC | 6.76 | 28.20 | 56.50 | 77.90 | 298.98 | 389.12 | 349.30 | 14.22 | |
| CNCs from chemical treatment of North African grass | — | — | — | — | 285 | — | 343 | 40.6 | [89] |
| CNCs synthesized from *Gliricidia sepium* via citric acid hydrolysis | — | — | — | — | — | — | 335 | ~15 | [88] |
| CNCs from Ethiopian lowland bamboo synthesized via citric acid/$H_2SO_4$ hydrolysis for 5 h at 80°C | — | — | — | — | 290 | 345 | 325 | — | [78] |

The major thermal decomposition stage occurs between 222 and 449°C and is related to depolymerization of biopolymers to produce volatiles such as carbon monoxide, methane, and carbondioxide, as well as the release of chemically bound water [90]. The weight loss of the samples in this region ranges from 73% to 90%. Additionally, the peak temperatures of all the samples are in the range of 325°C–351°C. All the CNCs exhibited a higher thermal resistance than the untreated sample, except DESCNC, which can be associated with dissolution of the crystalline regions of cellulose during acid hydrolysis, as observed by other authors [84]. This sample also had the lowest crystallinity, as shown in Table 7. Moreover, NaCNC has a higher degradation and onset temperature than UNNaCNC. The decrease in degradation temperature in this case is attributed to the gradual removal of hemicellulose and lignin and the increase in crystallinity, consistent with the results in Table 7 [77]. Furthermore, the presence of a carboxylic group in the UNNaCNC sample may be responsible for the lower onset and peak temperature, as noted by other authors [22]. However, the presence of lignin in micro-quantities has also been proven to contribute to a higher thermal stability of CNCs. The lignin acts as a natural compatibilizer, protecting the surface of the nanocellulose at high temperatures [91]. The excellent thermal stability of the NaCNC sample may have been influenced by this phenomenon.

From approximately 450°C–700°C, the mass loss is associated with combustion of residual compounds and lignin with char formation until a constant weight is achieved [75]. Char is produced due to the presence of lignin, hemicellulose, inorganic minerals, and stable oxides in the raw biomass source [92]. The final residue of the unbleached CNCs was also higher than that of the bleached CNCs at 700°C. This is associated with the chemical composition of the CNCs, with the unbleached CNCs containing more lignin, hemicellulose, and trace elements as shown in Table 2 and Table 5, in agreement with literature [93].

The residual char for the samples is also comparable to other lignocellulosic biomass previously reported [85]. The thermal profiles of all the samples are comparable to similar biomass published in literature [78, 88, 89].

## 4 | Conclusion

In this study, cellulose nanocrystals (CNCs) were successfully extracted from *Hyparrhenia filipendula* (also known as yellow thatching grass) through a series of pre-treatment procedures and Citric acid hydrolysis. The efficacy of two fractionation techniques was also compared: alkali treatment with NaOH and deep eutectic solvent of Ethylene glycol and Citric acid (1:2). The isolated CNCs were characterized for chemical and elemental composition, morphology, functional groups, crystallinity, and thermal stability. Based on the chemical composition, alkali fractionation was the most successful for delignification and depolymerization of hemicellulose, with the bleached sample achieving the greatest cellulose purity of 93%. The alterations in functional groups on the surface of the samples confirmed the changes in chemical composition with subsequent treatments.

The morphology of the CNCs fractionated with NaOH was needle-like, whereas the CNCs in the samples segregated with DES were rod-like. The average diameter of CNCs fractionated with DES was also greater than that of NaOH fractionated samples. The DES fractionated samples likewise had the lowest crystallinity, whereas the Alkali fractionated samples had the highest crystallinity. The highest crystallinity of the samples obtained in this study was 81% for the unbleached Alkali-pretreated CNC. This sample was also the only one with a dominant carboxylic functional group from the FTIR analysis. Furthermore, NaCNC, isolated using alkali fractionation, bleaching, and acid hydrolysis, had the highest thermal stability.

In general, the CNCs exhibited properties comparable to those found in the literature. Hence, the CNCs isolated from *Hyparrhenia filipendula* can be potentially employed for various applications, particularly as reinforcing agents in nanocomposites. Future work will focus on studying the reaction mechanisms to determine at which stage of CNC synthesis the DES is most effective. Additionally, a technoeconomic evaluation of DES integration in biorefineries should be conducted to evaluate its scalability and feasibility.

### Author Contributions

**Fildah Ayaa:** Conceptualization, Data curation, Formal analysis, Investigation, Methodology, Validation, Writing – original draft. **Michael Lubwama:** Conceptualization, Project administration, Resources, Supervision, Visualization, Writing – review and editing. **Samuel Ayodele Iwarere:** Conceptualization, Project administration, Supervision, Visualization, Writing – review and editing. **Michael Olawale Daramola:** Conceptualization, Funding acquisition, Project administration, Supervision, Visualization, Writing – review and editing. **John Baptist Kirabira:** Conceptualization, Funding acquisition, Project administration, Resources, Supervision, Writing – review and editing.

### Acknowledgments

This work was supported by the African Center of Excellence in Materials, Product Development and Nanotechnology (MAPRONANO ACE) funded by the World Bank and Government of Uganda [Project Identification P151847, IDA Number 5797-UG]. Additionally, Ayaa Fildah acknowledges the support she received from the Prof. Daramola Development Fund, which enabled her to complete her laboratory work at the University of Pretoria.

### Conflicts of Interest

The authors declare no conflicts of interest.

### Data Availability Statement

The datasets generated during and/or analyzed during the study are not publicly available due to Copyright regulations by Makerere University and the University of Pretoria, but are available from the corresponding author on reasonable request.

### References

1. C. S. Galik, M. E. Benedum, M. Kauffman, and D. R. Becker, "Opportunities and Barriers to Forest Biomass Energy: A Case Study of Four US States," *Biomass and Bioenergy* 148 (2021): 106035.

2. M. Muqeet, R. B. Mahar, T. A. Gadhi, and N. Ben Halima, "Insight Into Cellulose-Based-Nanomaterials—A Pursuit of Environmental Remedies," *International Journal of Biological Macromolecules* 163 (2020): 1480–1486.

3. S. H. Zainal, N. H. Mohd, N. Suhaili, F. H. Anuar, A. M. Lazim, and R. Othaman, "Preparation of Cellulose-Based Hydrogel: A Review," *Journal of Materials Research and Technology* 10 (2021): 935–952.

4. E. Lam and U. D. Hemraz, "Preparation and Surface Functionalization of Carboxylated Cellulose Nanocrystals," *Nanomaterials* 11, no. 7 (2021): 1641.

5. A. Durairaj, M. Maruthapandi, A. Saravanan, J. H. T. Luong, and A. Gedanken, "Cellulose Nanocrystals (CNC)-Based Functional Materials for Supercapacitor Applications," *Nanomaterials* 12, no. 11 (2022): 1828.

6. Q. Wang, X. Liu, Z. Qiang, et al., "Cellulose Nanocrystal Enhanced, High Dielectric 3D Printing Composite Resin for Energy Applications," *Composites Science and Technology* 227 (2022): 109601.

7. M. Okur and D. D. Eslek Koyuncu, "Investigation of Pretreatment Parameters in the Delignification of Paddy Husks With Deep Eutectic Solvents," *Biomass and Bioenergy* 142 (2020): 105811.

8. Y. Chen, Z. Yan, L. Liang, et al., "Comparative Evaluation of Organic Acid Pretreatment of Eucalyptus for Kraft Dissolving Pulp Production," *Materials* 13, no. 2 (2020): 361.

9. P. Mali and A. P. Sherje, "Cellulose Nanocrystals: Fundamentals and Biomedical Applications," *Carbohydrate Polymers* 275 (2022): 118668.

10. J. Sonyeam, R. Chaipanya, S. Suksomboon, et al., "Process Design for Acidic and Alcohol Based Deep Eutectic Solvent Pretreatment and High Pressure Homogenization of Palm Bunches for Nanocellulose Production," *Scientific Reports* 14, no. 1 (2024): 7550.

11. P. Panchal, E. Ogunsona, and T. Mekonnen, "Trends in Advanced Functional Material Applications of Nanocellulose," *Processes* 7, no. 1 (2018): 10.

12. L. P. Magagula, C. M. Masemola, M. A. Ballim, Z. N. Tetana, N. Moloto, and E. C. Linganiso, "Lignocellulosic Biomass Waste-Derived Cellulose Nanocrystals and Carbon Nanomaterials: A Review," *International Journal of Molecular Sciences* 23, no. 8 (2022): 4310.

13. H. Dai, J. Wu, H. Zhang, et al., "Recent Advances on Cellulose Nanocrystals for Pickering Emulsions: Development and Challenge," *Trends in Food Science & Technology* 102 (2020): 16–29.

14. D. Trache, M. H. Hussin, M. K. M. Haafiz, and V. K. Thakur, "Recent Progress in Cellulose Nanocrystals: Sources and Production," *Nanoscale* 9, no. 5 (2017): 1763–1786.

15. V. Tshivhase, R. Njinga, M. Mathuthu, and T. Dlamini, "Transfer Rates of 238U and 232Th for E. Globulus, A. Mearnsii, H. Filipendula and Hazardous Effects of the Usage of Medicinal Plants From Around Gold Mine Dump Environs," *International Journal of Environmental Research and Public Health* 12, no. 12 (2015): 15782–15793.

16. N. Ndwandwa, F. Ayaa, S. A. Iwarere, M. O. Daramola, and J. B. Kirabira, "Extraction and Characterization of Cellulose Nanofibers From Yellow Thatching Grass (Hyparrhenia filipendula) Straws via Acid Hydrolysis," *Waste and Biomass Valorization* 14, no. 8 (2023): 2599–2608.

17. Z. Kassab, I. Kassem, H. Hannache, R. Bouhfid, A. E. K. Qaiss, and M. El Achaby, "Tomato Plant Residue as New Renewable Source for Cellulose Production: Extraction of Cellulose Nanocrystals With Different Surface Functionalities," *Cellulose* 27, no. 8 (2020): 4287–4303.

18. Y. Tang, H. Yang, and S. Vignolini, "Recent Progress in Production Methods for Cellulose Nanocrystals: Leading to More Sustainable Processes," *Advanced Sustainable Systems* 6, no. 3 (2022): 2100100.

19. Q. Lin, H. Li, J. Ren, et al., "Production of Xylooligosaccharides by Microwave-Induced, Organic Acid-Catalyzed Hydrolysis of Different Xylan-Type Hemicelluloses: Optimization by Response Surface Methodology," *Carbohydrate Polymers* 157 (2017): 214–225.

20. W. Liu, H. Du, H. Liu, et al., "Highly Efficient and Sustainable Preparation of Carboxylic and Thermostable Cellulose Nanocrystals via FeCl3-catalyzed Innocuous Citric Acid Hydrolysis," *ACS Sustainable Chemistry & Engineering* 8, no. 44 (2020): 16691–16700.

21. T. J. Bondancia, J. de Aguiar, G. Batista, et al., "Production of Nanocellulose Using Citric Acid in a Biorefinery Concept: Effect of the Hydrolysis Reaction Time and Techno-Economic Analysis," *Industrial & Engineering Chemistry Research* 59, no. 25 (2020): 11505–11516.

22. H. Ji, Z. Xiang, H. Qi, T. Han, A. Pranovich, and T. Song, "Strategy Towards One-Step Preparation of Carboxylic Cellulose Nanocrystals and Nanofibrils With High Yield, Carboxylation and Highly Stable Dispersibility Using Innocuous Citric Acid," *Green Chemistry* 21, no. 8 (2019): 1956–1964.

23. C. Liu, H. Du, G. Yu, et al., "Simultaneous Extraction of Carboxylated Celulose Nanocrystals and Nanofibrils via Citric Acid Hydrolysis—A Sustainable Route," *Paper and Biomaterials* 2, no. 4 (2017): 19–26.

24. Z. Kassab, E. Syafri, Y. Tamraoui, H. Hannache, A. E. K. Qaiss, and M. El Achaby, "Characteristics of Sulfated and Carboxylated Cellulose Nanocrystals Extracted From Juncus Plant Stems," *International Journal of Biological Macromolecules* 154 (2020): 1419–1425.

25. M. V. C. Lozano, G. Sciutto, S. Prati, and R. Mazzeo, "Deep Eutectic Solvents: Green Solvents for the Removal of Degraded Gelatin on Cellulose Nitrate Cinematographic Films," *Heritage Science* 10, no. 1 (2022): 114.

26. A. M. da Costa Lopes, "Biomass Delignification With Green Solvents Towards Lignin Valorisation: Ionic Liquids Vs Deep Eutectic Solvents," *Acta Innovations*, no. 40 (2021): 64–78, https://doi.org/10.32933/ActaInnovations.40.5.

27. Q. Zhang, Z. Dai, L. Zhang, and Z. Wang, "Insights Into the Critical Role of Anions in Nanofibrillation of Cellulose in Deep Eutectic Solvents," *Cellulose* 32, no. 1 (2025): 97–114.

28. K. J. Nagarajan, N. R. Ramanujam, M. R. Sanjay, et al., "A Comprehensive Review on Cellulose Nanocrystals and Cellulose Nanofibers: Pretreatment, Preparation, and Characterization," *Polymer Composites* 42, no. 4 (2021): 1588–1630.

29. K. Dhali, M. Ghasemlou, F. Daver, P. Cass, and B. Adhikari, "A Review of Nanocellulose as a New Material Towards Environmental Sustainability," *Science of the Total Environment* 775 (2021): 145871.

30. A. A. Modenbach and S. E. Nokes, "Effects of Sodium Hydroxide Pretreatment on Structural Components of Biomass," *Transactions of the ASABE* 57, no. 4 (2014): 1187–1198.

31. Y. T. Tan, A. S. M. Chua, and G. C. Ngoh, "Deep Eutectic Solvent for Lignocellulosic Biomass Fractionation and the Subsequent Conversion to Bio-Based Products–A Review," *Bioresource Technology* 297 (2020): 122522.

32. D. Jose, Y. S. Cheng, S. M. K. Thiagamani, et al., "Integrating DES Pretreatment and Enzymatic Saccharification for Napier Grass Valorization," *Waste and Biomass Valorization*, ahead of print, June 2, 2025, https://doi.org/10.1007/s12649-025-03146-x.

33. J. Cai, J. Xue, Y. Li, L. Wei, N. Lin, and X. Zha, "Research Progress on High-Value-Added Application of Lignocellulosic Biomass Based on Deep Eutectic Solvent Pretreatment," *Biomass Conversion and Biorefinery* 14, no. 24 (2024): 30913–30928.

34. P. Li, C. Yang, Z. Jiang, Y. Jin, and W. Wu, "Lignocellulose Pretreatment by Deep Eutectic Solvents and Related Technologies: A Review," *Journal of Bioresources and Bioproducts* 8, no. 1 (2023): 33–44.

35. V. Jančíková and M. Jablonský, "Exploiting Deep Eutectic Solvent-Like Mixtures for Fractionation Biomass, and the Mechanism Removal of Lignin: A Review," *Sustainability* 16, no. 2 (2024): 504.

36. J. Tong, W. Hu, Y. Qin, and Y. Liu, "Deep Eutectic Solvent Pretreatment for Green Preparation of Nanocellulose," *Cellulose* 30, no. 8 (2023): 4773–4792.

37. C. Fang, M. H. Thomsen, C. G. Frankær, G. P. Brudecki, J. E. Schmidt, and I. M. AlNashef, "Reviving Pretreatment Effectiveness of Deep Eutectic Solvents on Lignocellulosic Date Palm Residues by Prior Recalcitrance Reduction," *Industrial & Engineering Chemistry Research* 56, no. 12 (2017): 3167–3174.

38. C. W. Gao, J. W. Allen, W. H. Green, and R. H. West, "Reaction Mechanism Generator: Automatic Construction of Chemical Kinetic Mechanisms," *Computer Physics Communications* 203 (2016): 212–225.

39. A. Sluiter, B. Hames, R. Ruiz, et al., "Determination of Structural Carbohydrates and Lignin in Biomass," *Laboratory analytical procedure* 1617, no. 1 (2008): 1–16.

40. C. Trilokesh and K. B. Uppuluri, "Isolation and Characterization of Cellulose Nanocrystals From Jackfruit Peel," *Scientific Reports* 9, no. 1 (2019): 16709.

41. J. Wongwatanapaiboon, K. Kangvansaichol, V. Burapatana, et al., "The Potential of Cellulosic Ethanol Production From Grasses in Thailand," *Journal of Biomedicine and Biotechnology* 2012 (2012): 1–10.

42. K. Przybysz, E. Małachowska, D. Martyniak, P. Boruszewski, H. Kalinowska, and P. Przybysz, "Production of Sugar Feedstocks for Fermentation Processes From Selected Fast Growing Grasses," *Energies* 12, no. 16 (2019): 3129.

43. B. Waliszewska, M. Grzelak, E. Gaweł, A. Spek-Dźwigała, A. Sieradzka, and W. Czekała, "Chemical Characteristics of Selected Grass Species From Polish Meadows and Their Potential Utilization for Energy Generation Purposes," *Energies* 14, no. 6 (2021): 1669.

44. O. Kamoga, J. Kirabira, and J. Byaruhanga, "Characterisation of Ugandan Selected Grasses and Tree Leaves for Pulp Extraction for Paper Industry," *International Journal of Scientific Technology Research* 2, no. 9 (2013): 146–154.

45. J. Zhang, H. Zhou, D. Liu, and X. Zhao, "Pretreatment of Lignocellulosic Biomass for Efficient Enzymatic Saccharification of Cellulose." *Lignocellulosic Biomass to Liquid Biofuels* (Elsevier, 2020), 17–65.

46. H. Xu, J. Peng, Y. Kong, et al., "Key Process Parameters for Deep Eutectic Solvents Pretreatment of Lignocellulosic Biomass Materials: A Review," *Bioresource Technology* 310 (2020): 123416.

47. R. Li, Y. Zheng, X. Zhao, et al., "Recent Advances in Biomass Pretreatment Using Biphasic Solvent Systems," *Green Chemistry* 25, no. 7 (2023): 2505–2523.

48. P. Bhagwat, A. Amobonye, S. Singh, and S. Pillai, "Deep Eutectic Solvents in the Pretreatment of Feedstock for Efficient Fractionation of Polysaccharides: Current Status and Future Prospects," *Biomass Conversion and Biorefinery* 12, no. Suppl 1 (2022): 171–195.

49. K. T. T. Amesho, Y. C. Lin, S. V. Mohan, S. Halder, V. K. Ponnusamy, and S. R. Jhang, "Deep Eutectic Solvents in the Transformation of Biomass into Biofuels and Fine Chemicals: A Review," *Environmental Chemistry Letters* 21, no. 1 (2023): 183–230.

50. S. Pongchaiphol, T. Preechakun, M. Raita, V. Champreda, and N. Laosiripojana, "Characterization of Cellulose–Chitosan-Based Materials From Different Lignocellulosic Residues Prepared by the Ethanosolv Process and Bleaching Treatment With Hydrogen Peroxide," *ACS Omega* 6, no. 35 (2021): 22791–22802.

51. S. Gan, S. Zakaria, P. Ng, C. H. Chia, and R. S. Chen, "Effect of Acid Hydrolysis and Thermal Hydrolysis on Solubility and Properties of Oil Palm Empty Fruit Bunch Fiber Cellulose Hydrogel," *BioResources* 11, no. 1 (2016): 126–139.

52. M. M. Haafiz, A. Hassan, A. K. HPS, et al., "Cellulose Nanowhiskers From Oil Palm Empty Fruit Bunch Biomass as Green Fillers." *Cellulose-Reinforced Nanofibre Composites* (Elsevier, 2017), 241–259.

53. N. A. Mohd Jamil, S. S. Jaffar, S. Saallah, et al., "Isolation of Cellulose Nanocrystals From Banana Peel Using One-Pot Microwave and Mild Oxidative Hydrolysis System," *Nanomaterials* 12, no. 19 (2022): 3537.

54. A. A. Modenbach and S. E. Nokes, "Effects of Sodium Hydroxide Pretreatment on Structural Components of Biomass," *ASABE* 57, no. 4 (2014): 1187–1198.

55. H. Qian, "Major Factors Influencing the Size Distribution Analysis of Cellulose Nanocrystals Imaged in Transmission Electron Microscopy," *Polymers* 13, no. 19 (2021): 3318.

56. A. Nang Vu, L. Hoang Nguyen, K. Yoshimura, T. Duy Tran, and H. Van Le, "Cellulose Nanocrystals Isolated From Sugarcane Bagasse Using the Formic/Peroxyformic Acid Process: Structural, Chemical, and Thermal Properties," *Arabian Journal of Chemistry* 17, no. 8 (2024): 105841.

57. P. A. Sinthiya, I. Johnson, H. J. Prabu, A. F. Sahayaraj, and M. T. Selvan, "Extraction of Cellulose Nanocrystals From Cissus Quadrangularis for Sustainable Biocomposite Production," *Biomass Conversion and Biorefinery* 15, no. 7 (2025): 10489–10501.

58. V. Muralidharan, S. Gochhayat, S. Palanivel, and B. Madhan, *Influence of Preparation Techniques of Cellulose II Nanocrystals as Reinforcement for Tannery Solid Waste-based Gelatin Composite Films*. 2022.

59. N. Johar, I. Ahmad, and A. Dufresne, "Extraction, Preparation and Characterization of Cellulose Fibres and Nanocrystals From Rice Husk," *Industrial Crops and Products* 37, no. 1 (2012): 93–99.

60. R. Radakisnin, M. S. Abdul Majid, M. R. M. Jamir, M. Jawaid, M. T. H. Sultan, and M. F. Mat Tahir, "Structural, Morphological and Thermal Properties of Cellulose Nanofibers From Napier Fiber (Pennisetum purpureum)," *Materials* 13, no. 18 (2020): 4125.

61. Z. Jebali, A. Nabili, H. Majdoub, and S. Boufi, "Cellulose Nanofibrils (CNFs) From Ammophila Arenaria, a Natural and a Fast Growing Grass Plant," *International Journal of Biological Macromolecules* 107 (2018): 530–536.

62. M. Chen, J. Parot, A. Mukherjee, et al., "Characterization of Size and Aggregation for Cellulose Nanocrystal Dispersions Separated by Asymmetrical-Flow Field-Flow Fractionation," *Cellulose* 27, no. 4 (2020): 2015–2028.

63. S. Głazowska, L. Baldwin, J. Mravec, et al., "The Impact of Silicon on Cell Wall Composition and Enzymatic Saccharification of Brachypodium Distachyon," *Biotechnology for Biofuels* 11, no. 1 (2018): 171.

64. R. Aryasena, N. Kusmono, and N. Umami, "Production of Cellulose Nanocrystals Extracted From Pennisetum Purpureum Fibers and Its Application as a Lubricating Additive in Engine Oil," *Heliyon* 8, no. 11 (2022): e11315.

65. S. Nasrazadani and S. Hassani, "Modern Analytical Techniques in Failure Analysis of Aerospace, Chemical, and Oil and Gas Industries," in *Handbook of Materials Failure Analysis with Case Studies From the Oil Gas Industry*, ed A. S. H. Makhlouf and M. Aliofkhazraei (2016), 39–54.

66. N. Qadi, K. Takeno, A. Mosqueda, M. Kobayashi, Y. Motoyama, and K. Yoshikawa, "Effect of Hydrothermal Carbonization Conditions on the Physicochemical Properties and Gasification Reactivity of Energy Grass," *Energy & Fuels* 33, no. 7 (2019): 6436–6443.

67. S. Garivait, J. P. Quisefit, P. de Chateaubourg, and G. Malingre, "Multi-Element Analysis of Plants by Wdxrf Using the Scattered Radiation Correction Method," *X-Ray Spectrometry* 26, no. 5 (1997): 257–264.

68. M. N. Khan, S. Ali, T. Yaseen, et al., "Assessment of Proximate and Nutritional Contents in Selected Weedy Grasses for Potential Use as Fodder in District Charsadda, KP: Assessment of Proximate and Nutritional Contents in Selected Weedy Grasses," *Proceedings of the Pakistan Academy of Sciences: B. Life Environmental Sciences* 57, no. 2 (2020): 83–94.

69. A. J. Metson, E. J. Gibson, J. L. Hunt, and W. M. H. Saunders, "Seasonal Variations in Chemical Composition of Pasture: III. Silicon, Aluminium, Iron, Zinc, Copper, and Manganese," *New Zealand Journal of Agricultural Research* 22, no. 2 (1979): 309–318.

70. J. Wang, Q. Wang, Y. Wu, et al., "Preparation of Cellulose Nanofibers From Bagasse by Phosphoric Acid and Hydrogen Peroxide Enables Fibrillation via a Swelling, Hydrolysis, and Oxidation Cooperative Mechanism," *Nanomaterials* 10, no. 11 (2020): 2227.

71. D. Haldar and M. K. Purkait, "Thermochemical Pretreatment Enhanced Bioconversion of Elephant Grass (Pennisetum Purpureum): Insight on the Production of Sugars and Lignin," *Biomass Conversion and Biorefinery* 12 (2020): 1–14.

72. A. C. W. Leung, S. Hrapovic, E. Lam, et al., "Characteristics and Properties of Carboxylated Cellulose Nanocrystals Prepared From a Novel One-Step Procedure," *Small* 7, no. 3 (2011): 302–305.

73. M. Sánchez-Gutiérrez, E. Espinosa, I. Bascón-Villegas, F. Pérez-Rodríguez, E. Carrasco, and A. Rodríguez, "Production of Cellulose Nanofibers From Olive Tree Harvest—A Residue With Wide Applications," *Agronomy* 10, no. 5 (2020): 696.

74. O. T. Abdulwahab, A. Ghazali, H. A. Khalil, et al., "Isolation and Characterization of Microcrystalline Cellulose From Oil Palm Fronds Using Chemo-Mechanical Process," *Wood Fiber Science* 48, no. 4 (2016): 260–270.

75. C.-M. Popescu, C. M. Tibirna, I. E. Raschip, M.-C. Popescu, P. Ander, and C. Vasile, "Bulk and Surface Characterization of Unbleached and Bleached Softwood Kraft Pulp Fibres," *Macromolecules* 9 (2008): 10.

76. S. A. Wahib, D. A. Da'na, and M. A. Al-Ghouti, "Insight into the Extraction and Characterization of Cellulose Nanocrystals From Date Pits," *Arabian Journal of Chemistry* 15, no. 3 (2022): 103650.

77. X. Wang, H. Le, Y. Guo, et al., "Preparation of Cellulose Nanocrystals From Jujube Cores by Fractional Purification," *Molecules* 27, no. 10 (2022): 3236.

78. L. A. Worku, R. K. Bachheti, and M. G. Tadesse, "Preparation and Characterization of Carboxylated Cellulose Nanocrystals From Oxytenanthera Abyssinica (Ethiopian Lowland Bamboo) Cellulose via Citric Acid Anhydrous Hydrolysis Catalyzed by Sulfuric Acid," *Biomass Conversion and Biorefinery* 14, no. 22 (2024): 28807–28823.

79. X. Yang, H. Xie, H. Du, et al., "Facile Extraction of Thermally Stable and Dispersible Cellulose Nanocrystals With High Yield via a Green and Recyclable FeCl3-catalyzed Deep Eutectic Solvent System," *ACS Sustainable Chemistry & Engineering* 7, no. 7 (2019): 7200–7208.

80. J. Coates, "Interpretation of Infrared Spectra, a Practical Approach," *Encyclopedia of Analytical Chemistry* 12 (2000): 10815–10837.

81. A. Fouda, G. Abdel-Maksoud, M. A. Abdel-Rahman, A. M. Eid, M. G. Barghoth, and M. A. H. El-Sadany, "Monitoring the Effect of Biosynthesized Nanoparticles Against Biodeterioration of Cellulose-Based Materials by Aspergillus Niger," *Cellulose* 26, no. 11 (2019): 6583–6597.

82. J. Gong, J. Li, J. Xu, Z. Xiang, and L. Mo, "Research on Cellulose Nanocrystals Produced From Cellulose Sources With Various Polymorphs," *RSC Advances* 7, no. 53 (2017): 33486–33493.

83. W.-C. Tu, L. Weigand, M. Hummel, H. Sixta, A. Brandt-Talbot, and J. P. Hallett, "Characterisation of Cellulose Pulps Isolated From Miscanthus Using a Low-Cost Acidic Ionic Liquid," *Cellulose* 27, no. 8 (2020): 4745–4761.

84. R. F. Kusmono, R. F. Listyanda, M. W. Wildan, and M. N. Ilman, "Preparation and Characterization of Cellulose Nanocrystal Extracted From Ramie Fibers by Sulfuric Acid Hydrolysis," *Heliyon* 6, no. 11 (2020): e05486.

85. B. Deepa, E. Abraham, N. Cordeiro, et al., "Utilization of Various Lignocellulosic Biomass for the Production of Nanocellulose: A Comparative Study," *Cellulose* 22, no. 2 (2015): 1075–1090.

86. Y. Chen, K. Shen, Z. He, et al., "Deep Eutectic Solvent Recycling to Prepare High Purity Dissolving Pulp," *Cellulose* 28, no. 18 (2021): 11503–11517.

87. T. Kurniawan, H. Sulistyarti, B. Rumhayati, and A. Sabarudin, "Preparation and Characteristics of Cellulose Nanocrystals (CNCs) Isolated From Palm Empty Bunches (PEB) at Various Temperatures and Concentrations of Sulfuric Acid Hydrolysis and Their Surface Modification With Aminomethylphosponic Acid (AMPA)," *Moroccan Journal of Chemistry* 12, no. 3 (2024): 931–969.

88. F. A. Fedin, H. Mohan, S. Thomas, and J. Kochupurackal, "Synthesis and Characterization of Nanocelluloses Isolated Through Acidic Hydrolysis and Steam Explosion of Gliricidia Sepium Plant Fiber," *Biomass Conversion and Biorefinery* 15, no. 6 (2025): 9097–9109.

89. F. Luzi, D. Puglia, F. Sarasini, et al., "Valorization and Extraction of Cellulose Nanocrystals From North African Grass: Ampelodesmos Mauritanicus (Diss)," *Carbohydrate Polymers* 209 (2019): 328–337.

90. F. Ayaa, M. Lubwama, J. B. Kirabira, and X. Jiang, "Potential of Invasive Shrubs for Energy Applications in Uganda," *Energy, Ecology and Environment* 7, no. 6 (2022): 563–576.

91. G. Kandhola, *Optimized Production and Evaluation of Cellulose Nanocrystals Derived From Pre-Extracted Kraft Pulp of Different Wood Species* (University of Arkansas, 2019).

92. M. Raza, B. Abu-Jdayil, F. Banat, and A. H. Al-Marzouqi, "Isolation and Characterization of Cellulose Nanocrystals From Date Palm Waste," *ACS Omega* 7, no. 29 (2022): 25366–25379.

93. O. Romruen, T. Karbowiak, W. Tongdeesoontorn, K. A. Shiekh, and S. Rawdkuen, "Extraction and Characterization of Cellulose From Agricultural By-Products of Chiang Rai Province, Thailand," *Polymers* 14, no. 9 (2022): 1830.